Open Access

Iraqi Journal of Industrial Research (IJOIR)

Journal homepage: http://ijoir.gov.iq

Protection Efficiency of Various Nickel Alloys Against Neutron, Gamma Radiation and X-rays Exposure

Kafa Khalaf Hammud*

Iraqi Atomic Energy Commission, Iraq

Article information

Article history:
Received: August, 08, 2025
Accepted: September, 15, 2025
Available online: December, 14, 2025

Keywords:
Nickel alloys,
Neutron,
Gamma radiation,
X-rays,
Phy-X software

Corresponding Author:
Kafa Khalaf Hammud
kafaakhalaf@gmail.com

DOI:
https://doi.org/10.53523/ijoirVol12I2ID594

This article is licensed under:
Creative Commons Attribution 4.0 International License.

Abstract

Six nickel alloys (Ni_3Al, NiAl, $Ni_{90}Cr_{10}$, $Ni_{80}Cr_{20}$, $Ni_{35}Cr_{20}Fe_{45}$, and $Ni_{60}Cr_{16}Fe_{34}$) varied in their chemical formulas, mole fractions (%) of each element, density, and Mean Atomic Number ($\bar{Z}$), alongside other chemical-physical properties were subjected to a prediction study depending on using NGCal and Phy-X software. Both free and friendly attenuation prediction software were chosen to calculate the attenuation factors against Neutron, Gamma radiation, and X-rays exposure. The calculated factors included Linear Attenuation Coefficient (LAC), Mass Attenuation Coefficient (MAC), Half and Tenth Value Layer (HVL and TVL), and Mean Free Path (MFP) by both Phy-X and online NGCAL software. NGCAL software was utilized to study the effect of photons at (0.1, 1, 15) MeV and neutrons [fast at 4 MeV and thermal at 25.4 meV). By using Phy-X software, energy range was (0.015-15) MeV, characteristic X-rays (K_α, K_β) included $_{29}$Cu, $_{37}$Rb, $_{42}$Mo, $_{47}$Ag, $_{56}$Ba, and $_{65}$Tb and radioactive isotopes were Am-241, Ba-133, Cd-109, Cs-137, Co-60, Eu-152, Fe-55, Na-22, and I-131. Additionally, protection efficiency (%) of each nickel alloy was calculated based on Lambert – Beer law by applying different thicknesses. The main aim of this prediction study is to provide workers that deal with Neutron, Gamma radiation, and X-rays particularly in the research, medical, industrial, and petroleum sectors most effective nickel alloy as a safe shielding material especially at high exposure energies. Both mathematical models indicated that Chromel ($Ni_{90}Cr_{10}$) as the highest density and high Nickel mole fraction exhibited the highest protection efficiency.

1. Introduction

Shielding material is the master key in the radiation protection issue by utilizing nontoxic and low-cost materials. In general, the shielding properties of neutrons are studied alongside gamma radiation. Protection against radiation or energetic particles plays a role in industry, medical diagnosis and therapy or other medical sectors, material analysis, military and the oil and gas sectors to safeguard workers from harmful effects. Gamma rays and neutrons are more challenging to stop compared to alpha and beta radiation. Neutrons are released in nuclear reactors. It is known the impact of radiation on humans and the environment especially tissues and organ: burns, DNA or nervous system damage, is well known. Such harmful effects may be arising from direct

or indirect interactions with X-rays or radioactive sources, including Naturally Occurred Radioactive Materials (NORM). Many articles have evaluated the X-rays, gamma radiation, and neutron shielding parameters in alloys, metals, composites, and other types of materials, such as lead-copper binary alloys or ternary alloys, brasses, silver and palladium alloys, aluminum alloys, zinc, yttrium, and Mg-Y-Zn alloys. Additionally, polymers and polymer concretes, nickel, chromium and tungsten stainless steels, zirconium materials, and ceramics are included [1-30].

Here, a theoretical study is presented to evaluate the ability of several nickel alloys to protect against Neutron, Gamma radiation, and X-rays exposure. These nickel alloys include Ni_3Al, NiAl, $Ni_{90}Cr_{10}$, $Ni_{80}Cr_{20}$, $Ni_{35}Cr_{20}Fe_{45}$, and $Ni_{60}Cr_{16}Fe_{34}$ which vary in their chemical-physical properties including chemical formulas, mole fractions (%) of each element, density, and Mean Atomic Number ($\bar{Z}$). The predictive evaluation is depending on using freely and friendly NGCal and Phy-X software presented by Linear Attenuation Coefficient (LAC), Mass Attenuation Coefficient (MAC), Half and Tenth Value Layer (HVL and TVL), and Mean Free Path (MFP) as attention factors.

NGCal software utilizes photons at (0.1, 1, 15) MeV and neutrons [fast at 4 MeV and thermal at 25.4 meV). By using Phy-X software, energy range was (0.015-15) MeV, characteristic X-rays (K_α, K_β) included $_{29}$Cu, $_{37}$Rb, $_{42}$Mo, $_{47}$Ag, $_{56}$Ba, and $_{65}$Tb and radioactive isotopes were Am-241, Ba-133, Cd-109, Cs-137, Co-60, Eu-152, Fe-55, Na-22, and I-131.

For a better understanding of which nickel alloy serves as the most efficient protector, the protection efficiency (%) of each nickel alloy was calculated based on Lambert-Beer law by applying different thicknesses. Protection efficiency is a physical concept used to calculate the ability of the tested material to protect human from a specific threat; here gamma, X-rays, neutron; and this percentage is a quantitative measure describes the success the tested protection material or method. The main aim of this predictive study is to provide workers who deal with neutron, gamma radiation, and X-rays-particularly in the research, medical, industrial, and petroleum sectors-with the most effective nickel alloy as a safe shielding material, especially at high exposure energies [20-33].

2. Experimental and Theoretical Part

Six nickel alloys with different chemical compositions, in addition to varying physical properties, were selected for this predictive study (Table 1). These selected nickel alloys are known for their unique characteristics. For example, nickel aluminide refers to a nickel- aluminum alloy that exists as an intermetallic compound, either Ni_3Al or NiAl, both of which exhibit high strength and corrosion resistance. Ni_3Al is a nickel-based super-alloy (γ'-phase, brittle polycrystalline material) while NiAl demonstrates good thermal conductivity and oxidation resistance, making it suitable for coatings in gas turbines, treating furnaces, and jet engines. This NiAl generally suffers from brittleness below 330°C and a rapid loss of strength above 550°C [30, 31].

Additionally, $Ni_{90}Cr_{10}$ is one of the nickel-chromium alloy products used in the heating industry (up to 1250°C) and possesses high resistivity, oxidation resistance, ductility, and weldability. It is a positive conductor for ANSI thermocouples (Type E and K) where this temperature sensor is fitted to the standards set by the American National Standards Institute (ANSI) [32]. $Ni_{80}Cr_{20}$ is an alloy with good thermal properties, including fusion, diffusivity, and conductivity, and its composition reflects intermediate resistivity [33].

Table (1): Nickel alloys specifications.

Code	Chemical formula,	Mole fraction, %		Density, gm/cm^3	Mean Atomic Number, $\bar{Z}$
S1	Ni_3Al	Ni	0.75	7.5	٢٤.25
		Al	0.25		
S2	NiAl	Ni	0.50	5.85	20.5
		Al	0.50		
S3	$Ni_{90}Cr_{10}$	Ni	0.90	8.5	27.6
		Cr	0.10		
S4	$Ni_{80}Cr_{20}$	Ni	0.80	8.3	٢7.2
		Cr	0.20		
S5	$Ni_{35}Cr_{20}Fe_{45}$	Ni	0.35	7.9	26.3
		Cr	0.20		
		Fe	0.45		
S6	$Ni_{60}Cr_{16}Fe_{34}$	Ni	0.5455	8.2	29.48
		Cr	0.1455		
		Fe	0.3091		

NGCal (Figure 1) and Phy-X (Figure 2), as free and friendly attenuation prediction software, were chosen to calculate the attenuation factors against Neutron, Gamma radiation, and X-rays exposure [28, 29].

The calculated factors were Linear Attenuation Coefficient (LAC), Mass Attenuation Coefficient (MAC), Half Value Layer (HVL), Tenth Value Layer (TVL), and Mean Free Path (MFP) by both Phy-X and online NGCAL software. NGCAL software was used to study the effect of photons at (0.1, 1, 15) MeV and neutrons [fast at 4 MeV and thermal at 25.4 meV) (Figure 1). While Phy-X software was applied for both X-rays sources for both K_α and K_β and isotopes based on gamma photon energy range (0.015 -15) MeV (Figure 2) as below. The general behavior (LAC, MAC, HVL, TVL, and MEP, and other Phy-X calculated parameters) of each tested alloy was varied according to its chemical composition and density (Figures 3-8).

Selected energy range: (0.015-15) MeV
Characteristic X-rays (K_α, K_β): $_{29}$Cu, $_{37}$Rb, $_{42}$Mo, $_{47}$Ag, $_{56}$Ba, and $_{65}$Tb

Radioactive Isotopes:
Am-241: (0.01381 – 0.103) MeV, Ba-133: (0.03082 – 0.38839) MeV, Cd-109: (0.0255 - 0.08804) MeV, Cs-137: (0.2835 – 0.6617) MeV, Co-60: (0.3471 -2.506) MeV, Eu-152: (0.0395 – 1.458) MeV, Fe-55: (0.005888 – 0.006536) MeV, Na-22: (0.511, 1.273) MeV, and I-131: (0.364 -0.723) MeV.

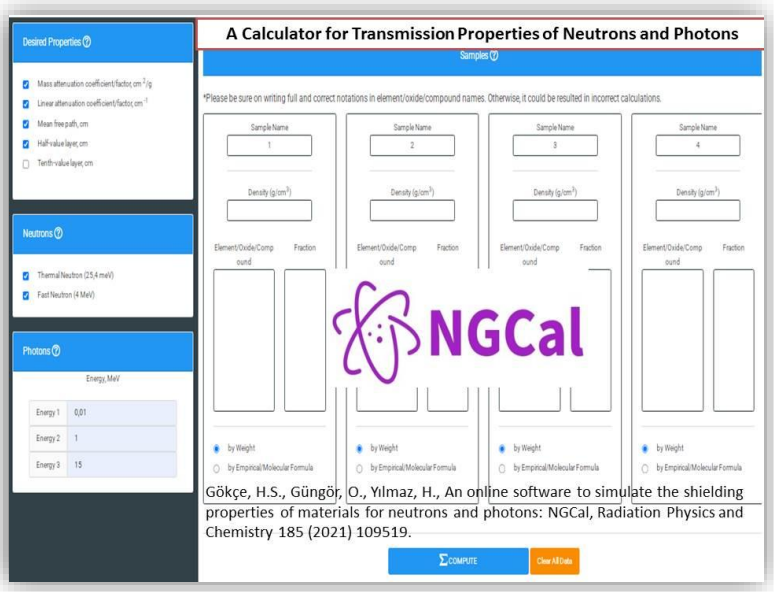

Figure (1): NGCal software and the selected calculation parameters.

Figure (2): Applied energy range by the friendly Photon Shielding and Dosimetry (PSD) software (Phy-x).

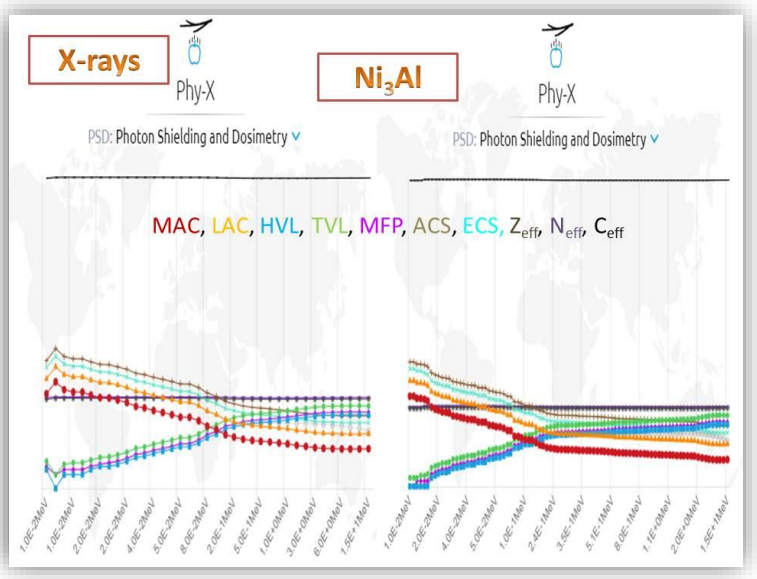

Figure (3): Ni_3Al behavior against X-rays and Radioactive isotopes according to Phy-X shielding parameters.

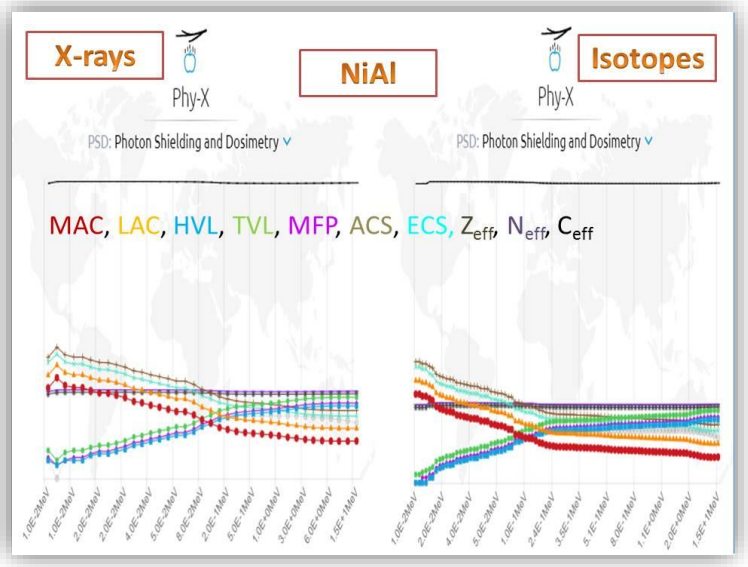

Figure (4): NiAl behavior against X-rays and Radioactive isotopes according to Phy-X shielding parameters.

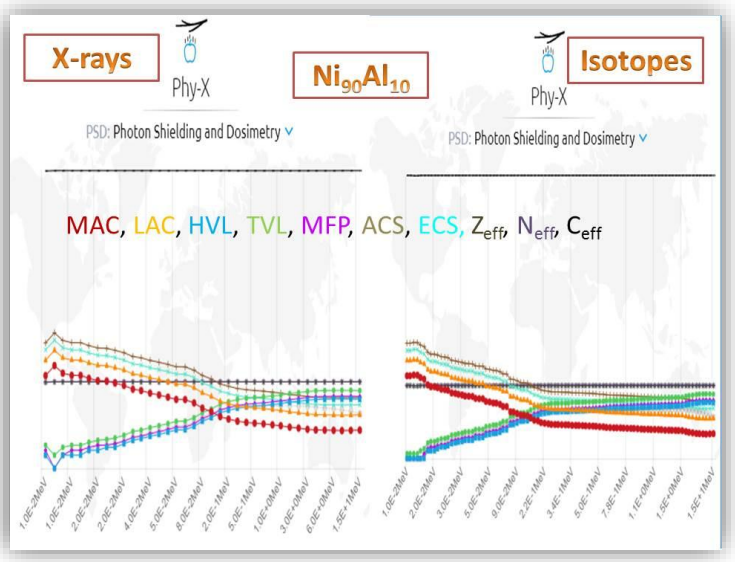

Figure (5): $Ni_{90}Al_{10}$ behavior against X-rays and Radioactive isotopes according to Phy-X shielding parameters.

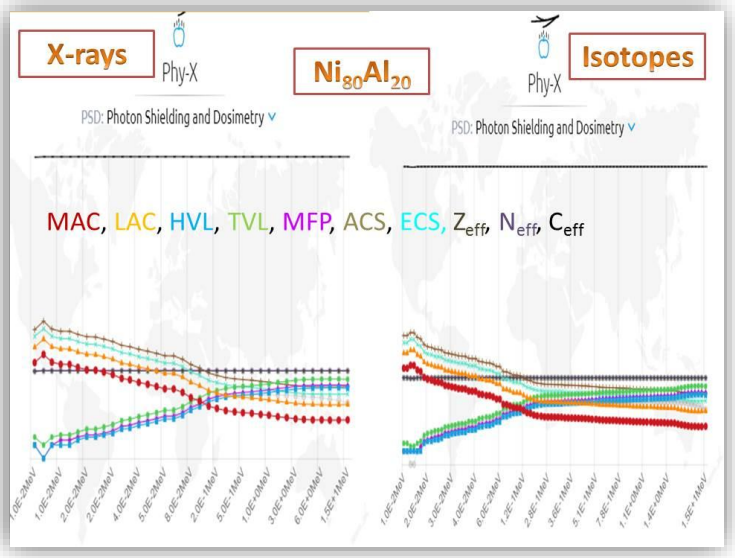

Figure (6): $Ni_{80}Al_{20}$ behavior against X-rays and Radioactive isotopes according to Phy-X shielding parameters.

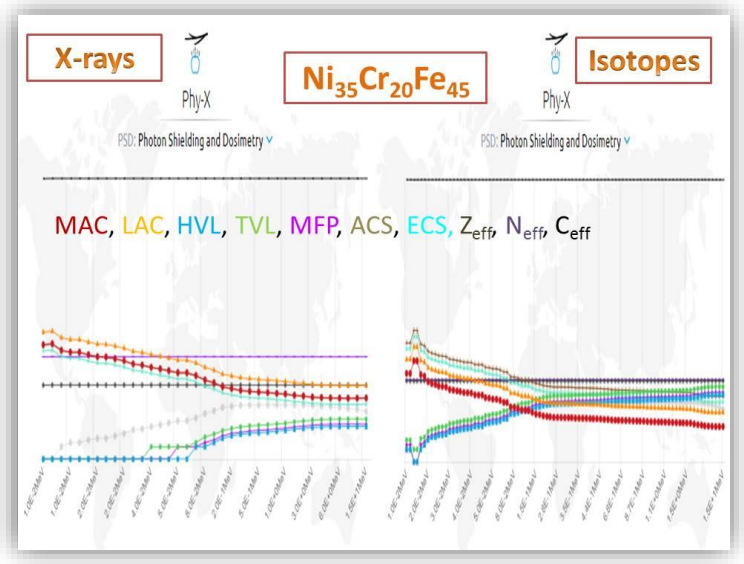

Figure (7): $Ni_{35}Cr_{20}Fe_{45}$ behavior against X-rays and Radioactive isotopes according to Phy-X shielding parameters.

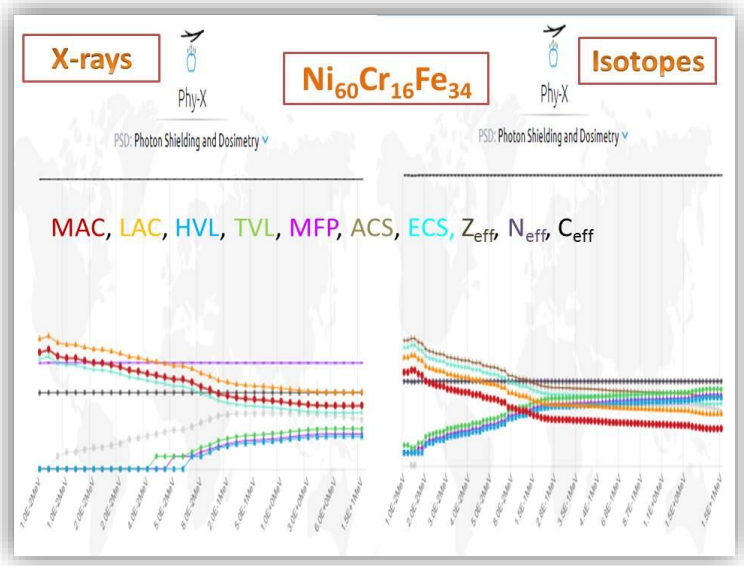

Figure (8): $Ni_{60}Cr_{16}Fe_{34}$ behavior against X-rays and Radioactive isotopes according to Phy-X shielding parameters.

Table (2): Linear Attenuation coefficient of each alloy against Characteristic X-rays (K_α, K_β): ^{29}Cu, ^{37}Rb,^{42}Mo, ^{47}Ag, ^{56}Ba, and ^{65}Tb calculated by Phy-X software.

Energy, MeV	*X-ray source*	S1	S2	S3	S4	S5	S6
8.04E-03	*Cu (29)*	367.116	287.145	566.429	704.199	1247.067	1572.354
8.91E-03	*Cu (29)*	1851.788	1186.285	2300.509	2174.530	2067.794	1899.029
1.34E-02	*Rb (37)*	641.073	408.757	797.817	753.530	711.108	649.851
1.50E-02	*Rb (37)*	471.007	300.080	585.974	552.990	521.946	476.660
1.50E-02		468.439	298.440	582.775	549.964	519.088	474.043
1.74E-02	*Mo (42)*	310.257	197.477	385.897	363.882	343.117	312.938
1.96E-02	*Mo (42)*	224.124	142.574	278.734	262.717	247.426	225.418

Energy, MeV	*X-ray source*	S1	S2	S3	S4	S5	S6
2.00E-02		212.854	135.396	264.712	249.485	234.922	213.992
2.21E-02	*Ag (47)*	161.314	102.588	200.580	188.980	177.813	161.852
2.49E-02	*Ag (47)*	115.540	73.480	143.616	135.263	127.193	115.697
3.00E-02		68.393	43.532	84.942	79.967	75.154	68.313
3.21E-02	*Ba (56)*	56.723	36.125	70.420	66.289	62.290	56.609
3.64E-02	*Ba (56)*	39.723	25.341	49.267	46.374	43.566	39.585
4.00E-02		30.483	19.483	37.772	35.555	33.400	30.347
4.45E-02	*Tb (65)*	22.695	14.547	28.085	26.442	24.840	22.574
5.00E-02		16.459	10.595	20.329	19.148	17.995	16.364
5.04E-02	*Tb (65)*	16.123	10.382	19.912	18.755	17.627	16.030
6.00E-02		10.104	6.568	12.428	11.719	11.032	10.052
8.00E-02		4.952	3.300	6.027	5.702	5.392	4.940
1.00E-01		3.057	2.093	3.677	3.493	3.322	3.065
1.50E-01		1.573	1.139	1.845	1.769	1.704	1.596
2.00E-01		1.151	0.859	1.329	1.282	1.245	1.177
3.00E-01		0.854	0.654	0.974	0.945	0.923	0.879
4.00E-01		0.727	0.562	0.826	0.802	0.786	0.750
5.00E-01		0.650	0.504	0.736	0.716	0.702	0.671
6.00E-01		0.594	0.462	0.673	0.654	0.642	0.614
8.00E-01		0.516	0.402	0.584	0.568	0.557	0.534
1.00E+00		0.462	0.360	0.522	0.508	0.498	0.477
1.50E+00		0.376	0.293	0.425	0.414	0.406	0.389
2.00E+00		0.328	0.255	0.372	0.362	0.355	0.340
3.00E+00		0.279	0.215	0.317	0.308	0.302	0.289
4.00E+00		0.255	0.195	0.291	0.283	0.277	0.264
5.00E+00		0.242	0.184	0.278	0.269	0.264	0.251
6.00E+00		0.235	0.178	0.271	0.263	0.257	0.244
8.00E+00		0.230	0.172	0.267	0.258	0.252	0.240
1.00E+01		0.230	0.170	0.268	0.259	0.253	0.240
1.50E+01		0.238	0.173	0.279	0.270	0.262	0.248

Table (3): Linear Attenuation coefficient of each alloy against Radioactive isotopes: ^{241}Am, ^{133}Ba, ^{109}Cd, ^{137}Cs, ^{60}Co, ^{152}Eu, ^{55}Fe, ^{22}Na, and ^{131}I calculated by Phy-X software.

Energy, MeV	*Isotope source*	S1	S2	S3	S4	S5	S6
5.89E-03	*Fe (55)*	867.344	683.917	940.234	883.217	749.246	827.483
5.90E-03	*Fe (55)*	862.915	680.395	935.462	878.732	745.435	823.277
6.49E-03	*Fe (55)*	662.909	521.616	1045.496	1319.701	1200.091	1100.030
6.54E-03	*Fe (55)*	650.092	511.448	1027.359	1298.199	1180.787	1081.690
1.38E-02	*Am (241)*	586.991	374.184	730.440	689.725	594.770	650.952
1.50E-02		468.439	298.440	582.775	549.964	474.043	519.088
2.00E-02		212.854	135.396	264.712	249.485	213.992	234.922
2.21E-02	*Ag (47)*	161.314	102.588	200.580	188.980	161.852	177.813
2.31E-02	*Cd (109)*	142.567	90.663	177.250	166.977	142.931	157.070

Energy, MeV	*Isotope source*	S1	S2	S3	S4	S5	S6
2.50E-02	*Cd (109)*	114.248	72.658	142.008	133.747	114.396	125.765
2.55E-02	*Cd (109)*	108.068	68.731	134.317	126.497	108.177	118.939
2.63E-02	*Am (241)*	98.658	62.752	122.606	115.458	98.712	108.548
3.00E-02		68.393	43.532	84.942	79.967	68.313	75.154
3.08E-02	*Ba (133)*	63.389	40.356	78.715	74.102	63.293	69.637
3.22E-02	*Am (241)*	56.129	35.749	69.681	65.593	56.014	61.636
3.32E-02	*Am (241)*	51.409	32.754	63.807	60.062	51.284	56.435
3.50E-02	*Ba (133)*	44.314	28.253	54.980	51.751	44.180	48.621
3.54E-02	*Ba (133)*	42.922	27.370	53.247	50.120	42.786	47.088
3.58E-02	*Ba (133)*	41.588	26.524	51.588	48.558	41.451	45.620
3.95E-02	*Eu (152)*	31.573	20.174	39.127	36.831	31.436	34.598
4.00E-02		30.483	19.483	37.772	35.555	30.347	33.400
4.01E-02	*Eu (152)*	30.229	19.322	37.456	35.258	30.094	33.121
4.59E-02	*Eu (152)*	20.809	13.351	25.739	24.236	20.695	22.769
4.70E-02	*Eu (152)*	19.451	12.491	24.050	22.647	19.341	21.277
4.96E-02	*Ba (133)*	16.805	10.814	20.760	19.553	16.708	18.374
5.00E-02		16.459	10.595	20.329	19.148	16.364	17.995
5.32E-02	*Ba (133)*	13.940	8.998	17.196	16.202	13.860	15.233
5.95E-02	*Am (241)*	10.310	6.698	12.684	11.959	10.256	11.257
6.00E-02		10.104	6.568	12.428	11.719	10.052	11.032
8.00E-02		4.952	3.300	6.027	5.702	4.940	5.392
8.10E-02	*Ba (133)*	4.812	3.210	5.853	5.539	4.802	5.238
8.80E-02	*Cd (109)*	3.990	2.688	4.833	4.580	3.988	4.340
9.90E-02	*Am (241)*	3.121	2.134	3.756	3.568	3.128	3.391
1.00E-01		3.057	2.093	3.677	3.493	3.065	3.322
1.03E-01	*Am (241)*	2.885	1.983	3.463	3.292	2.894	3.133
1.22E-01	*Eu (152)*	2.135	1.503	2.537	2.421	2.153	2.316
1.50E-01		1.573	1.139	1.845	1.769	1.596	1.704
1.61E-01	*Ba (133)*	1.446	1.055	1.688	1.622	1.470	1.565
2.00E-01		1.151	0.859	1.329	1.282	1.177	1.245
2.23E-01	*Ba (133)*	1.048	0.789	1.205	1.164	1.074	1.133
2.45E-01	*Eu (152)*	0.978	0.741	1.121	1.084	1.004	1.057
2.76E-01	*Ba (133)*	0.899	0.686	1.027	0.996	0.925	0.972
2.84E-01	*Cs (137)*	0.885	0.676	1.010	0.979	0.910	0.956
2.84E-01	*I (131)*	0.884	0.675	1.009	0.978	0.909	0.955
2.96E-01	*Eu (152)*	0.862	0.660	0.983	0.953	0.887	0.931
3.00E-01		0.854	0.654	0.974	0.945	0.879	0.923
3.03E-01	*Ba (133)*	0.849	0.651	0.968	0.939	0.874	0.918
3.44E-01	*Eu (152)*	0.789	0.607	0.897	0.871	0.813	0.852
3.47E-01	*Co (60)*	0.785	0.605	0.893	0.867	0.809	0.848
3.56E-01	*Ba (133)*	0.774	0.597	0.880	0.854	0.798	0.836
3.65E-01	*I (131)*	0.764	0.589	0.869	0.843	0.788	0.825
3.84E-01	*Ba (133)*	0.743	0.574	0.844	0.820	0.767	0.803

Energy, MeV	*Isotope source*	S1	S2	S3	S4	S5	S6
4.00E-01		0.727	0.562	0.826	0.802	0.750	0.786
4.11E-01	*Eu (152)*	0.717	0.555	0.814	0.791	0.740	0.774
4.44E-01	*Eu (152)*	0.690	0.534	0.782	0.760	0.712	0.745
5.00E-01		0.650	0.504	0.736	0.716	0.671	0.702
5.11E-01	*Na (22)*	0.643	0.499	0.728	0.708	0.664	0.694
6.00E-01		0.594	0.462	0.673	0.654	0.614	0.642
6.37E-01	*I (131)*	0.577	0.449	0.653	0.635	0.596	0.623
6.62E-01	*Cs (137)*	0.567	0.441	0.641	0.623	0.585	0.612
6.78E-01	*Eu (152)*	0.560	0.436	0.633	0.616	0.579	0.604
6.89E-01	*Eu (152)*	0.556	0.432	0.628	0.611	0.574	0.600
7.23E-01	*I (131)*	0.543	0.422	0.614	0.597	0.561	0.586
7.79E-01	*Eu (152)*	0.523	0.407	0.591	0.575	0.541	0.565
8.00E-01		0.516	0.402	0.584	0.568	0.534	0.557
8.26E-01	*Co (60)*	0.508	0.396	0.574	0.559	0.525	0.549
8.67E-01	*Eu (152)*	0.496	0.387	0.561	0.546	0.513	0.536
9.64E-01	*Eu (152)*	0.471	0.367	0.532	0.517	0.486	0.508
1.00E+00		0.462	0.360	0.522	0.508	0.477	0.498
1.01E+00	*Eu (152)*	0.461	0.359	0.520	0.506	0.476	0.497
1.09E+00	*Eu (152)*	0.443	0.345	0.500	0.487	0.458	0.478
1.09E+00	*Eu (152)*	0.442	0.345	0.499	0.486	0.457	0.477
1.11E+00	*Eu (152)*	0.437	0.341	0.494	0.481	0.452	0.472
1.17E+00	*Co (60)*	0.426	0.332	0.481	0.468	0.440	0.459
1.28E+00	*Na (22)*	0.408	0.318	0.461	0.448	0.422	0.440
1.30E+00	*Eu (152)*	0.404	0.315	0.457	0.444	0.418	0.436
1.33E+00	*Co (60)*	0.399	0.311	0.451	0.439	0.412	0.431
1.41E+00	*Eu (152)*	0.388	0.303	0.438	0.427	0.401	0.419
1.46E+00	*Eu (152)*	0.381	0.297	0.431	0.419	0.394	0.412
1.50E+00		0.376	0.293	0.425	0.414	0.389	0.406
2.00E+00		0.328	0.255	0.372	0.362	0.340	0.355
2.51E+00	*Co (60)*	0.298	0.231	0.338	0.329	0.309	0.323
3.00E+00		0.279	0.215	0.317	0.308	0.289	0.302
4.00E+00		0.255	0.195	0.291	0.283	0.264	0.277
5.00E+00		0.242	0.184	0.278	0.269	0.251	0.264
6.00E+00		0.235	0.178	0.271	0.263	0.244	0.257
8.00E+00		0.230	0.172	0.267	0.258	0.240	0.252
1.00E+01		0.230	0.170	0.268	0.259	0.240	0.253
1.50E+01		0.238	0.173	0.279	0.270	0.248	0.262

Table (4): Linear and Mass Attenuation coefficients of each alloy against neutron (thermal and fast) and photon (0.01, 1, and 15) MeV calculated by NGCal software.

ID	Linear attenuation coefficient. cm^{-1}		Linear attenuation coefficient. cm^{-1}			Mass attenuation coefficient. cm^2/g		Mass attenuation coefficient. cm^2/g		
	Neutrons		Photons (MeV)			Neutrons		Photons (MeV)		
	Thermal (25.4 meV)	Fast (4 MeV)	0.01	1	15	Thermal (25.4 meV)	Fast (4 MeV)	0.01	1	15
S1	0.652	0.347	1385.360	0.462	0.238	0.087	0.046	184.715	0.062	0.032
S2	0.408	0.214	885.926	0.360	0.173	0.070	0.037	151.440	0.062	0.030
S3	0.809	0.426	1716.660	0.522	0.279	0.095	0.050	201.960	0.061	0.033
S4	0.754	0.389	1617.836	0.507	0.269	0.091	0.047	194.920	0.061	0.032
S5	0.478	0.196	1403.356	0.477	0.248	0.060	0.025	177.640	0.060	0.031
S6	0.593	0.275	1532.505	0.498	0.262	0.072	0.034	186.891	0.061	0.032

Table (5): Mean Free Path, Half-value layer, and tenth – value layer of each alloy against photon (0.01, 1, and 15) MeV calculated by NGCal software.

ID	Mean free path (for Photons). cm			Half-value layer (for Photons). Cm			Tenth-value layer (for Photons). cm		
	0.01 MeV	1 MeV	15 MeV	0.01 MeV	1 MeV	15 MeV	0.01 MeV	1 MeV	15 MeV
S1	0.001	2.165	4.205	0.001	1.501	2.915	0.002	4.985	9.683
S2	0.001	2.777	5.764	0.001	1.925	3.995	0.003	6.394	13.272
S3	0.001	1.917	3.587	0.000	1.329	2.486	0.001	4.414	8.259
S4	0.001	1.971	3.719	0.000	1.366	2.578	0.001	4.537	8.562
S5	0.001	2.096	4.035	0.000	1.453	2.797	0.002	4.826	9.290
S6	0.001	2.007	3.821	0.000	1.391	2.649	0.002	4.622	8.799

3. Results and Discussion

Because Gamma rays and X-rays are not electrically charged radiation, they can penetrate the target substance. So, exposure must be controlled by a suitable shield. Attenuation performance has been evaluated by theoretical studies that may be companied by experiments. Experimental studies are highly regarded in nuclear science and technology. To minimize time, cost, errors, toxicity, … etc., it is preferred to evaluate attenuation characteristics using computer-based models, including ParShield, XCOM, GRASP, NGCAL, Phy-X/PSD, Geant4, and others. These simulation models are designed to calculate the attenuation parameters. An excellent radiation attenuator needs to be with high density and Effective Atomic Number [1, 2, 3, 8, 19, 20, 23, 28, 29, 34, 35, 36].

As shown in theoretical calculations, X-rays and gamma rays may be released from many sources including characteristic X-rays (K_α, K_β): ^{29}Cu, ^{37}Rb, ^{42}Mo, ^{47}Ag, ^{56}Ba, and ^{65}Tb beside radioactive isotopes: ^{241}Am, ^{133}Ba, ^{109}Cd, ^{137}Cs, ^{60}Co, ^{152}Eu, ^{55}Fe, ^{22}Na, and ^{131}I. Natural gamma rays may be released from Natural Occurred Radioactive Materials (NORM) that workers exposed to it in petroleum wells and gas sites besides oil - gas associated industries. Here, protection of workers is more than necessary issue and choosing the shielding material mainly depends on health – environmental considerations as well as their structural, chemical, and physical properties. Selection steps are more effectively to be done through theoretical calculations then followed by experimental studies [38 - 42].

Both energetic rays are absorbed by a number of materials, some of which were mentioned in the introduction section. In our presented study, different nickel alloys are subjected to free, user-friendly software (NGCal and Phy-X) [28, 29]. Both mathematical calculations require the chemical formula, density, and energy to obtain the attenuation behavior of each alloy (numerical data). Here, the calculated factors are LAC, MAC, HVL, and MFP according to the energy values mentioned in the experimental section (see Figures 3-10).

LAC (μ, cm^{-1}) is a fundamental attenuation factor related to the Lambert-Beer equation (Table 2, equation 1). It is used to calculate other shielding parameters such as MAC (μ_m, cm^2/g), HVL, and TVL (equations 2, 3, 4, 5). Both TVL and HVL represent the thickness (cm) needed to reduce the exposed radiation intensity by one tenth and one half, respectively. The MEP parameter marks the average distance when two photons (or particles) incident on the tested materials.

From equations (2-5), there is an inverse relationship between LAC and the tested parameters (TVL, HVL, or MFP), while MAC has a proportional relationship with LAC. MAC is also influenced by the density of the tested shielding material (equation 2). MAC outlines the interaction probability between photons or neutrons and the medium or the tested material (mass unit/area unit). The linear attenuation coefficient (LAC, μ) is used to obtain these parameters as follows:

$$I = I_o \times e^{-\mu x} \quad \text{..... (1)}$$

$$\mu_m = \mu/\rho \quad \text{..... (2)}$$

$$TVL = \ln 10/\mu \quad \text{..... (3)}$$

$$HVL = \ln 2/\mu \quad \text{..... (4)}$$

$$MFP = 1/\mu \quad \text{..... (5)}$$

Where, I: attenuated intensity, I_o: un-attenuated intensity, x: thickness (cm), ρ: density (gm/cm^3).

Tables (2-5) and Figures (3-10) show that LAC and MAC decreased with increasing of energy and best shielding material was (S3, $Ni_{90}Cr_{10}$) where the sequence of nickel alloys according to LAC and MAC by both tested software as bellow.

LAC (photons): S2 < S1 < S5 < S6 < S4 < S3
LAC (thermal neutrons, 25.4 MeV): S2 < S5< S6 < S1 < S4 < S3
LAC (fast neutrons, 4 MeV): S5 < S2 < S6 < S1 < S4 < S3

MAC (photon): S2 < S6 < S1 < S4 < S5 < S3
MAC (NGCal, thermal neutron, 25.4 MeV): S5<S2<S6< S1 < S4 < S3
MAC (NGCal, fast neutron, 4 MeV): S5 < S6 < S2 < S1 < S4 < S3
HVL, TVL, MFP (photon): S3 < S4 < S6 < S5 < S1 < S2

The difference between the LAC and MAC sequences is related to the influence of density (see Equation 2). Additionally, the MAC sequence is affected by material density, incident photon energy, and/or incident neutron energy (25.4 meV or 4 MeV). The LAC, MAC, HVL, TVL, and MFP sequences are the same in NGCal and Phy-X software. Furthermore, the difference in each calculated parameter via NGCal and Phy-X was less than 1% [37]. The differences were calculated using Equation 6, and the differences in some data were tabulated (Table 6). LAC data in Table (6) were not selected at 0.01 MeV because LAC was not found at this energy (Phy-X software) to compare and calculate the percentage of difference (Δ%).

$$\Delta\% = (\mu_{Phy\text{-}X} - \mu_{NGCal})/\mu_{Phys\text{-}X}) \times 100 \quad \text{..... (6)}$$

Table (6): Phy-X and NGCal Percentage of Difference (Δ%) depending on LAC data.

ID	NGCal Linear attenuation coefficient. cm^{-1}		Phy-X Linear attenuation coefficient. cm^{-1}		Percentage of Difference (Δ%)	
	1 MeV	15 MeV	1 MeV	15 MeV	1 MeV	15 MeV
S1	0.462	0.238	0.462	0.238	0	0
S2	0.36	0.173	0.360	0.173	0	0
S3	0.522	0.279	0.522	0.279	0	0

S4	0.507	0.269	0.508	0.270	0.19685	0.37037
S5	0.477	0.248	0.477	0.248	0	0
S6	0.498	0.262	0.498	0.22	0	-19.0909

The obtained results by both software give the workers in any related sectors numerical data to choose which nickel alloy can be applied to each incident photon or neutron Figures (3-10).

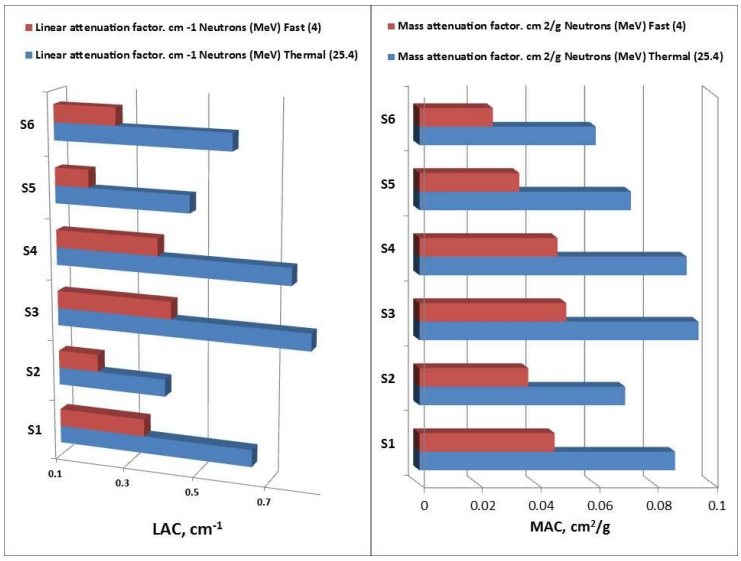

Figure (9): LAC and MAC for incident neutron according to NGCal software.

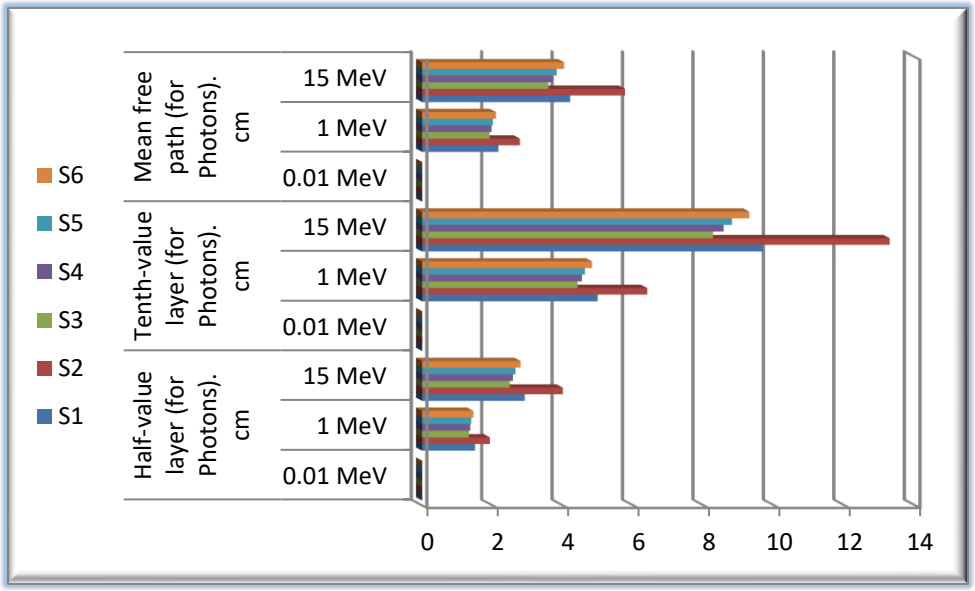

Figure (10): HVL, TVL, and MFP for incident neutron according to NGCal software.

In this study, the Protection Efficiency (PE, %) was another shielding parameter that calculated depending on the LAC data and the Beer–Lamberts law (Equation 1). In practical conditions, Equation (1) parameters (x, I, and I_o) can be directly measured. So, PE% is easily to be calculated by simple mathematical modification (equations (7-10)) as below [37]:

$$I/Io = e^{-\mu x} \text{ ..... (7)}$$

$$\textbf{Protection Efficiency (PE, \%)} = ((I_o - I)/I_o) \times 100 \ldots\ldots\ldots \textbf{(8)}$$

$$\textbf{Protection Efficiency (PE, \%)} = ((1 - (I/I_o)) \times 100 \ldots\ldots\ldots \textbf{(9)}$$

$$\textbf{Protection Efficiency (PE, \%)} = (1-(e^{-\mu x})) \times 100 \ldots\ldots\ldots \textbf{(10)}$$

To do theoretical calculations, the thickness (x) is numerically absent; therefore, the PE% can be calculated by assuming the thickness. This PE% is very important character to see the whole image by anyone and clearly identifying which material is more suitable or efficient for neutrons, X-rays, or gamma rays' attenuation. Additionally, Equation 10 is suitable to estimate the PE% at any energy of these neutrons, X-rays, or gamma rays from any source and any tested thickness by using the LAC (μ) data from computerized model.

In this study, PE% was calculated for each case with thickness (0.1 cm and 1 cm) as shown in Tables (7, 8, & 9) where PE% has a proportional relationship with thickness increasing while inverse relationship was found between energy and PE%. Additionally, the highest PE% was found $Ni_{90}Cr_{10}$ (S3) among other nickel alloys.

From Table (7), PE% showed that all tested nickel alloys with 100% protection against X-rays emitted from $_{29}Cu$, $_{37}Rb$, and $_{42}Mo$ with thickness = 0.1 cm while X-rays emission $_{29}Cu$, $_{37}Rb$, $_{42}Mo$, $_{47}Ag$, $_{56}Ba$, and $_{65}Tb$ (0.0445 MeV) from can be completely attenuated with thickness = 1 cm. with thickness (1 cm). At the highest tested energy (15 MeV), the maximum PE% was 24.346% with thickness=1 cm belongs to $Ni_{90}Cr_{10}$ (S3).

Radioactive isotopes (^{55}Fe) and (^{241}Am, 1.38 $x10^{-2}$MeV) emission can be completely attenuated by all tested alloys with thickness = 0.1 cm while other isotopes ^{47}Ag, ^{109}Cd, ^{241}Am ((0.0263 and 0.0332) MeV), ^{133}Ba ((0.0308, 0.0350, 0.0354, 0.0358) MeV), and ^{152}Eu ((0.0395, 0.0401, 0.0459, and 0.047) MeV) can be completely attenuated by all tested alloys with thickness = 1 cm (Table 8).

The radiation released from ^{133}Ba with energies (0.049 and 0.0532) MeV was completely attenuated (PE%=100%) by all tested alloys except S2 (x= 1cm). Additionally, $Ni_{90}Cr_{10}$ (S3) showed PE% = 100% where energy not exceeded 0.06MeV and thickness (x=1 cm) as shown in Table (8).

From Table (8), this superior protection alloy - $Ni_{90}Cr_{10}$ (S3, Figure 11) with thickness (1 cm) showed PE% more than 45% to protect workers from ^{137}Cs radiation (0.284 and 0.662) MeV. Additionally, workers with radioactive ^{60}Co ((0.347 – 2.51) MeV) need thickness of S3 more than (1 cm) where this nickel alloy attenuated ^{60}Co radiation ((0.347 – 2.51) MeV from (59.057 – 28.80) % (Table 8).

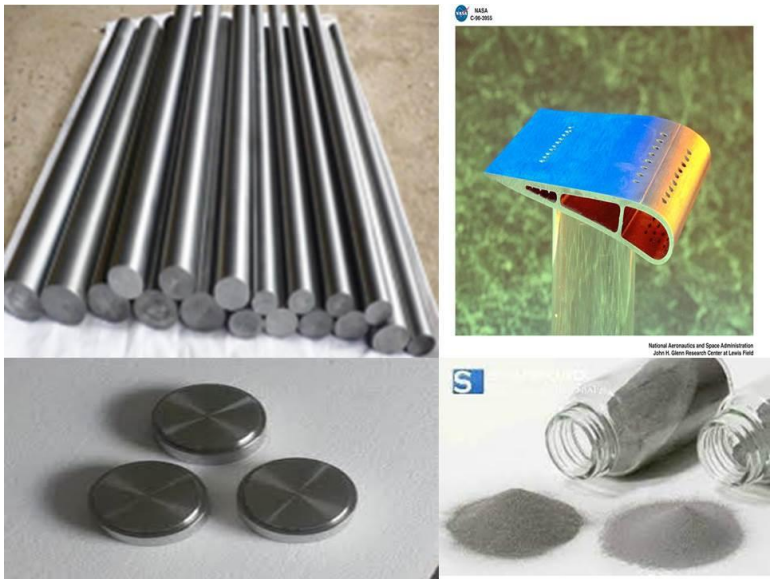

Figure (11): Nickel Aluminide.

From all calculated characters, the content of nickel in any tested alloy has the major influence when comparing S1 with S2, (S3-S6), or S5 with S6. The effect of the mean atomic number and density, which is related to the Ni content, has a proportional relationship with any calculated character. At this point, increasing thickness gives a high PE% against neutron and photon exposure, especially at low energy, as shown in Table (9) based on LAC-NGCal (Table 9).

For a more detailed comparison, LAC and PE% of these tested nickel alloys (thickness x = 1 cm) were evaluated alongside their basic metals (Ni, Al, Cr, and Fe) and Pb via NGCal software (Table 10). Lead was added because of its widespread use as a shielding material. Through numerical assessment of the tested alloys and these elements against thermal neutrons, fast neutrons, and photons (0.01, 1, and 15 MeV), general observations of LAC and PE% can be noted as follows:

Thermal neutrons: **Ni** > Cr > Fe > Al > Pb ; **S3** > S4 > S1 > S6 > S5 > S2
Fast neutrons: **Ni** > Cr > Fe > Al > Pb; **S3** > S4 > S1 > S6 > S2 > S5
Photons: **Pb** > Ni > Fe > Cr > Al ; **S3** > S4 > S6 > S5 > S1 > S2
Summary between tested nickel alloys, their basic metal, and lead:
Thermal and fast neutrons: **Ni** > **S3** > S4 > S1 > S6 > S5 > S2 > Cr > Fe > Al > Pb
Photons: **Pb** > Ni > **S3** > S4 > S6 > S5 > Fe > S1 > Cr > S2 > Al

Table (7): Protection Efficiency (PE%) of each alloy against X-rays exposure depending (LAC, Phy-X).

Energy, MeV	*X-ray source*	Thickness (x=0.1 cm)						thickness (x= 1 cm)					
		S1	S2	S3	S4	S5	S6	S1	S2	S3	S4	S5	S6
8.04E-03	*Cu (29)*	100	100	100	100	100	100	100	100	100	100	100	100
8.91E-03	*Cu (29)*	100	100	100	100	100	100	100	100	100	100	100	100
1.34E-02	*Rb (37)*	100	100	100	100	100	100	100	100	100	100	100	100
1.50E-02	*Rb (37)*	100	100	100	100	100	100	100	100	100	100	100	100
1.50E-02		100	100	100	100	100	100	100	100	100	100	100	100
1.74E-02	*Mo (42)*	100	100	100	100	100	100	100	100	100	100	100	100
1.96E-02	*Mo (42)*	100	100	100	100	100	100	100	100	100	100	100	100
2.00E-02		100	100	100	100	100	100	100	100	100	100	100	100
2.21E-02	*Ag (47)*	100	99.996	100	100	100	100	100	100	100	100	100	100
2.49E-02	*Ag (47)*	99.999	99.936	100	100	100	99.999	100	100	100	100	100	100
3.00E-02		99.893	98.713	99.980	99.966	99.946	99.892	100	100	100	100	100	100
3.21E-02	*Ba (56)*	99.656	97.302	99.913	99.868	99.803	99.652	100	100	100	100	100	100
3.64E-02	*Ba (56)*	98.117	92.067	99.275	99.032	98.718	98.091	100	100	100	100	100	100
4.00E-02		95.256	85.748	97.711	97.143	96.456	95.191	100	100	100	100	100	100
4.45E-02	*Tb (65)*	89.664	76.653	93.970	92.894	91.659	89.538	100	100	100	100	100	100
5.00E-02		80.716	65.337	86.904	85.263	83.462	80.532	100	99.997	100	100	100	100
5.04E-02	*Tb (65)*	80.057	64.591	86.347	84.672	82.842	79.871	100	99.997	100	100	100	100
6.00E-02		63.593	48.149	71.142	69.022	66.819	63.403	99.996	99.860	100	99.999	99.998	99.996
8.00E-02		39.055	28.108	45.267	43.459	41.679	38.982	99.293	96.312	99.759	99.666	99.545	99.285

Energy, MeV	*X-ray source*	Thickness (x=0.1 cm)						thickness (x= 1 cm)					
		S1	S2	S3	S4	S5	S6	S1	S2	S3	S4	S5	S6
1.00E-01		26.339	18.885	30.768	29.482	28.266	26.398	95.297	87.668	97.470	96.959	96.392	95.335
1.50E-01		14.555	10.765	16.848	16.214	15.667	14.752	79.258	67.986	84.197	82.950	81.805	79.729
2.00E-01		10.872	8.231	12.445	12.032	11.706	11.104	68.368	57.641	73.526	72.252	71.206	69.180
3.00E-01		8.186	6.331	9.281	9.017	8.817	8.415	57.429	48.004	62.243	61.132	60.267	58.480
4.00E-01		7.012	5.465	7.928	7.707	7.559	7.226	51.664	42.993	56.220	55.157	54.434	52.763
5.00E-01		6.293	4.915	7.096	6.910	6.779	6.490	47.795	39.589	52.097	51.130	50.441	48.880
6.00E-01		5.767	4.515	6.509	6.331	6.218	5.955	44.789	36.998	48.982	48.004	47.376	45.882
8.00E-01		5.029	3.940	5.673	5.522	5.418	5.200	40.310	33.102	44.234	43.334	42.707	41.374
1.00E+00		4.515	3.536	5.086	4.953	4.858	4.658	36.998	30.232	40.667	39.830	39.226	37.936
1.50E+00		3.690	2.887	4.161	4.055	3.979	3.815	31.340	25.398	34.623	33.900	33.369	32.227
2.00E+00		3.227	2.518	3.652	3.555	3.488	3.343	27.964	22.508	31.065	30.372	29.883	28.823
3.00E+00		2.751	2.127	3.120	3.033	2.975	2.849	24.346	19.346	27.167	26.508	26.066	25.099
4.00E+00		2.518	1.931	2.868	2.790	2.732	2.605	22.508	17.717	25.248	24.648	24.195	23.203
5.00E+00		2.391	1.823	2.742	2.654	2.605	2.479	21.494	16.806	24.270	23.586	23.203	22.198
6.00E+00		2.323	1.764	2.674	2.596	2.537	2.410	20.943	16.306	23.738	23.126	22.663	21.651
8.00E+00		2.274	1.705	2.635	2.547	2.489	2.371	20.547	15.802	23.433	22.740	22.276	21.337
1.00E+01		2.274	1.686	2.644	2.557	2.498	2.371	20.547	15.634	23.509	22.818	22.353	21.337
1.50E+01		2.352	1.715	2.751	2.664	2.586	2.450	21.180	15.886	24.346	23.662	23.049	21.964

Table (8): Protection Efficiency (PE%) of each alloy against various radioactive isotopes exposure depending on LAC values (Phy-X).

Energy, MeV	*Isotope source*	Thickness (x=0.1 cm)						Thickness (x= 1 cm)					
		S1	S2	S3	S4	S5	S6	S1	S2	S3	S4	S5	S6
5.89E-03	*Fe (55)*	100	100	100	100	100	100	100	100	100	100	100	100
5.90E-03	*Fe (55)*	100	100	100	100	100	100	100	100	100	100	100	100
6.49E-03	*Fe (55)*	100	100	100	100	100	100	100	100	100	100	100	100
6.54E-03	*Fe (55)*	100	100	100	100	100	100	100	100	100	100	100	100
1.38E-02	*Am (241)*	100	100	100	100	100	100	100	100	100	100	100	100
1.50E-02		100	100	100	100	100	100	100	100	100	100	100	100
2.00E-02		100	100	100	100	100	100	100	100	100	100	100	100
2.21E-02	*Ag (47)*	100	99.996	100	100	100	100	100	100	100	100	100	100
2.31E-02	*Cd (109)*	100	99.988	100	100	100	100	100	100	100	100	100	100
2.50E-02	*Cd (109)*	99.999	99.930	100	100	99.999	100	100	100	100	100	100	100
2.55E-02	*Cd (109)*	99.998	99.896	100	100	99.998	99.999	100	100	100	100	100	100
2.63E-02	*Am (241)*	99.995	99.812	100	99.999	99.995	99.998	100	100	100	100	100	100
3.00E-02		99.893	98.713	99.980	99.966	99.892	99.946	100	100	100	100	100	100
3.08E-02	*Ba*	99.823	98.232	99.962	99.939	99.822	99.905	100	100	100	100	100	100

Energy, MeV	*Isotope source*	Thickness (x=0.1 cm)						Thickness (x= 1 cm)					
		S1	S2	S3	S4	S5	S6	S1	S2	S3	S4	S5	S6
	(133)												
3.22E-02	*Am (241)*	99.635	97.198	99.906	99.858	99.631	99.790	100	100	100	100	100	100
3.32E-02	*Am (241)*	99.415	96.220	99.831	99.754	99.407	99.646	100	100	100	100	100	100
3.50E-02	*Ba (133)*	98.810	94.071	99.591	99.434	98.794	99.227	100	100	100	100	100	100
3.54E-02	*Ba (133)*	98.633	93.524	99.513	99.334	98.614	99.098	100	100	100	100	100	100
3.58E-02	*Ba (133)*	98.437	92.952	99.425	99.222	98.416	98.956	100	100	100	100	100	100
3.95E-02	*Eu (152)*	95.746	86.700	98.001	97.486	95.687	96.856	100	100	100	100	100	100
4.00E-02		95.256	85.748	97.711	97.143	95.191	96.456	100	100	100	100	100	100
4.01E-02	*Eu (152)*	95.134	85.517	97.638	97.057	95.068	96.356	100	100	100	100	100	100
4.59E-02	*Eu (152)*	87.518	73.687	92.376	91.140	87.375	89.740	100	100	100	100	100	100
4.70E-02	*Eu (152)*	85.703	71.324	90.973	89.614	85.545	88.089	100	100	100	100	100	100
4.96E-02	*Ba (133)*	81.372	66.088	87.457	85.848	81.190	84.077	100	99.998	100	100	100	100
5.00E-02		80.716	65.337	86.904	85.263	80.532	83.462	100	99.997	100	100	100	100
5.32E-02	*Ba (133)*	75.192	59.335	82.086	80.214	74.993	78.201	100	99.988	100	100	100	100
5.95E-02	*Am (241)*	64.335	48.819	71.872	69.757	64.142	67.557	99.997	99.877	100	99.999	99.996	99.999
6.00E-02		63.593	48.149	71.142	69.022	63.403	66.819	99.996	99.860	100	99.999	99.996	99.998
8.00E-02		39.055	28.108	45.267	43.459	38.982	41.679	99.293	96.312	99.759	99.666	99.285	99.545
8.10E-02	*Ba (133)*	38.196	27.458	44.306	42.530	38.134	40.773	99.187	95.964	99.713	99.607	99.179	99.469
8.80E-02	*Cd (109)*	32.901	23.570	38.326	36.745	32.888	35.209	98.150	93.198	99.204	98.975	98.146	98.696
9.90E-02	*Am (241)*	26.809	19.217	31.312	30.009	26.860	28.759	95.589	88.164	97.662	97.179	95.619	96.633
1.00E-01		26.339	18.885	30.768	29.482	26.398	28.266	95.297	87.668	97.470	96.959	95.335	96.392
1.03E-01	*Am (241)*	25.061	17.988	29.270	28.050	25.129	26.897	94.415	86.234	96.866	96.282	94.465	95.641
1.22E-01	*Eu (152)*	19.225	13.955	22.408	21.502	19.370	20.674	88.176	77.754	92.090	91.117	88.386	90.133
1.50E-01		14.555	10.765	16.848	16.214	14.752	15.667	79.258	67.986	84.197	82.950	79.729	81.805
1.61E-01	*Ba (133)*	13.463	10.013	15.532	14.973	13.671	14.487	76.449	65.181	81.511	80.250	77.007	79.091
2.00E-01		10.872	8.231	12.445	12.032	11.104	11.706	68.368	57.641	73.526	72.252	69.180	71.206
2.23E-01	*Ba (133)*	9.950	7.587	11.352	10.988	10.183	10.712	64.936	54.570	70.031	68.777	65.836	67.793
2.45E-01	*Eu (152)*	9.317	7.142	10.605	10.273	9.552	10.031	62.394	52.336	67.405	66.176	63.359	65.250
2.76E-01	*Ba (133)*	8.598	6.630	9.760	9.480	8.835	9.263	59.302	49.641	64.192	63.065	60.347	62.167
2.84E-01	*Cs (137)*	8.470	6.537	9.607	9.326	8.698	9.117	58.729	49.135	63.578	62.431	59.748	61.557
2.84E-01	*I (131)*	8.461	6.527	9.598	9.317	8.689	9.108	58.687	49.084	63.542	62.394	59.707	61.519
2.96E-01	*Eu (152)*	8.259	6.387	9.362	9.090	8.488	8.890	57.768	48.315	62.581	61.442	58.811	60.584
3.00E-01		8.186	6.331	9.281	9.017	8.415	8.817	57.429	48.004	62.243	61.132	58.480	60.267

Energy, MeV	*Isotope source*	Thickness (x=0.1 cm)						Thickness (x= 1 cm)					
		S1	S2	S3	S4	S5	S6	S1	S2	S3	S4	S5	S6
3.03E-01	*Ba (133)*	8.140	6.303	9.226	8.963	8.369	8.771	57.216	47.848	62.016	60.898	58.272	60.068
3.44E-01	*Eu (152)*	7.587	5.889	8.579	8.341	7.808	8.167	54.570	45.502	59.221	58.147	55.647	57.344
3.47E-01	*Co (60)*	7.550	5.871	8.543	8.305	7.771	8.130	54.388	45.393	59.057	57.979	55.470	57.173
3.56E-01	*Ba (133)*	7.448	5.795	8.424	8.186	7.670	8.020	53.884	44.954	58.522	57.429	54.977	56.656
3.65E-01	*I (131)*	7.355	5.720	8.323	8.084	7.578	7.919	53.420	44.512	58.063	56.958	54.525	56.177
3.84E-01	*Ba (133)*	7.161	5.578	8.094	7.873	7.383	7.716	52.432	43.673	57.001	55.957	53.560	55.202
4.00E-01		7.012	5.465	7.928	7.707	7.226	7.559	51.664	42.993	56.220	55.157	52.763	54.434
4.11E-01	*Eu (152)*	6.919	5.399	7.818	7.605	7.133	7.448	51.179	42.593	55.692	54.661	52.289	53.884
4.44E-01	*Eu (152)*	6.667	5.200	7.522	7.318	6.872	7.179	49.842	41.374	54.251	53.233	50.934	52.527
5.00E-01		6.293	4.915	7.096	6.910	6.490	6.779	47.795	39.589	52.097	51.130	48.880	50.441
5.11E-01	*Na (22)*	6.228	4.868	7.021	6.835	6.424	6.705	47.429	39.286	51.713	50.737	48.521	50.043
6.00E-01		5.767	4.515	6.509	6.331	5.955	6.218	44.789	36.998	48.982	48.004	45.882	47.376
6.37E-01	*I (131)*	5.607	4.391	6.321	6.153	5.786	6.040	43.842	36.173	47.952	47.006	44.899	46.367
6.62E-01	*Cs (137)*	5.512	4.314	6.209	6.040	5.682	5.936	43.278	35.661	47.323	46.367	44.289	45.773
6.78E-01	*Eu (152)*	5.446	4.266	6.134	5.974	5.626	5.861	42.879	35.338	46.900	45.990	43.954	45.338
6.89E-01	*Eu (152)*	5.408	4.228	6.087	5.927	5.578	5.824	42.650	35.079	46.634	45.719	43.673	45.119
7.23E-01	*I (131)*	5.285	4.132	5.955	5.795	5.456	5.692	41.900	34.427	45.882	44.954	42.936	44.345
7.79E-01	*Eu (152)*	5.096	3.988	5.739	5.588	5.266	5.493	40.726	33.436	44.623	43.730	41.783	43.164
8.00E-01		5.029	3.940	5.673	5.522	5.200	5.418	40.310	33.102	44.234	43.334	41.374	42.707
8.26E-01	*Co (60)*	4.953	3.883	5.578	5.437	5.115	5.342	39.830	32.699	43.673	42.822	40.844	42.247
8.67E-01	*Eu (152)*	4.839	3.796	5.456	5.314	5.001	5.219	39.104	32.091	42.936	42.074	40.130	41.492
9.64E-01	*Eu (152)*	4.601	3.603	5.181	5.039	4.744	4.953	37.562	30.719	41.257	40.369	38.492	39.830
1.00E+00		4.515	3.536	5.086	4.953	4.658	4.858	36.998	30.232	40.667	39.830	37.936	39.226
1.01E+00	*Eu (152)*	4.505	3.526	5.067	4.934	4.648	4.849	36.935	30.163	40.548	39.710	37.874	39.165
1.09E+00	*Eu (152)*	4.333	3.391	4.877	4.753	4.477	4.668	35.789	29.178	39.347	38.553	36.745	37.998
1.09E+00	*Eu (152)*	4.324	3.391	4.868	4.744	4.467	4.658	35.725	29.178	39.286	38.492	36.682	37.936
1.11E+00	*Eu (152)*	4.276	3.353	4.820	4.696	4.419	4.610	35.403	28.894	38.982	38.184	36.365	37.625
1.17E+00	*Co (60)*	4.171	3.265	4.696	4.572	4.305	4.486	34.688	28.251	38.184	37.375	35.596	36.808
1.28E+00	*Na (22)*	3.998	3.130	4.505	4.381	4.132	4.305	33.502	27.240	36.935	36.110	34.427	35.596
1.30E+00	*Eu (152)*	3.959	3.101	4.467	4.343	4.094	4.266	33.236	27.021	36.682	35.853	34.164	35.338
1.33E+00	*Co (60)*	3.911	3.062	4.410	4.295	4.036	4.218	32.901	26.729	36.301	35.532	33.768	35.014
1.41E+00	*Eu (152)*	3.806	2.985	4.285	4.180	3.931	4.103	32.159	26.140	35.467	34.754	33.035	34.230
1.46E+00	*Eu*	3.738	2.926	4.218	4.103	3.863	4.036	31.682	25.696	35.014	34.230	32.565	33.768

Energy, MeV	*Isotope source*	Thickness (x=0.1 cm)						Thickness (x= 1 cm)					
		S1	S2	S3	S4	S5	S6	S1	S2	S3	S4	S5	S6
	(152)												
1.50E+00		3.690	2.887	4.161	4.055	3.815	3.979	31.340	25.398	34.623	33.900	32.227	33.369
2.00E+00		3.227	2.518	3.652	3.555	3.343	3.488	27.964	22.508	31.065	30.372	28.823	29.883
2.51E+00	*Co (60)*	2.936	2.284	3.324	3.236	3.043	3.178	25.770	20.626	28.680	28.036	26.582	27.603
3.00E+00		2.751	2.127	3.120	3.033	2.849	2.975	24.346	19.346	27.167	26.508	25.099	26.066
4.00E+00		2.518	1.931	2.868	2.790	2.605	2.732	22.508	17.717	25.248	24.648	23.203	24.195
5.00E+00		2.391	1.823	2.742	2.654	2.479	2.605	21.494	16.806	24.270	23.586	22.198	23.203
6.00E+00		2.323	1.764	2.674	2.596	2.410	2.537	20.943	16.306	23.738	23.126	21.651	22.663
8.00E+00		2.274	1.705	2.635	2.547	2.371	2.489	20.547	15.802	23.433	22.740	21.337	22.276
1.00E+01		2.274	1.686	2.644	2.557	2.371	2.498	20.547	15.634	23.509	22.818	21.337	22.353
1.50E+01		2.352	1.715	2.751	2.664	2.450	2.586	21.180	15.886	24.346	23.662	21.964	23.049

Table (9): Protection Efficiency of each alloy against neutron (thermal and fast) and photon (0.01, 1, and 15) MeV depending on LAC values (NGCal).

ID	PE%, x=0.1cm					PE%, x=1cm				
	Neutrons (MeV)		Photons (MeV)			Neutrons (MeV)		Photons (MeV)		
	Thermal (25.4)	Fast (4)	0.01	1	15	Thermal (25.4)	Fast (4)	0.01	1	15
S1	**6.3120**	**3.4105**	**100**	**4.5149**	**2.3519**	**47.8997**	**29.3195**	**100**	**36.9978**	**21.1797**
S2	**3.9979**	2.1173	100	3.5360	1.7151	33.5021	19.2652	100	30.2324	15.8862
S3	**7.7714**	4.1705	100	5.0861	2.7514	55.4697	34.6884	100	40.6667	24.3460
S4	**7.2628**	3.8153	100	4.9436	2.6541	52.9519	32.2266	100	39.7700	23.5857
S5	**4.6676**	1.9409	100	4.6580	2.4495	37.9978	17.7988	100	37.9358	21.9640
S6	**5.7576**	2.7125	100	4.8580	2.5860	44.7333	24.0428	100	39.2255	23.0489

Table (10): LAC and PE% of the basic metals of the tested alloys by NGCal software.

ID	Linear attenuation factor. cm^{-1}					PE%, x= 1 cm				
	Neutrons		Photons			Neutrons		Photons		
	Thermal (25.4 meV)	Fast (4 MeV)	0.01 MeV	1 MeV	15 MeV	Thermal (25.4 meV)	Fast (4 MeV)	0.01 MeV	1 MeV	15 MeV
Al	0.0144	0.0005	70.8210	0.1659	0.0593	1.4311	0.0482	100	15.2905	5.7543
Pb	0.0057	0.0001	1481.0040	0.8054	0.6416	0.5718	0.0099	100	55.3076	47.3560
Cr	0.4036	0.1513	989.6040	0.4234	0.2085	33.2056	14.0437	100	34.5185	18.8189
Fe	0.2509	0.0339	1340.9160	0.4712	0.2430	22.1884	3.3334	100	37.5752	21.5753
Ni	0.8856	0.4752	1861.5630	0.5487	0.2957	58.7516	37.8253	100	42.2283	25.5999

From equations (3, 4, 5, and 10), PE% can be calculated from TVL, HVL, and MEP values as below:

$$\textbf{Protection Efficiency (PE, \%)} = (1-(e^{-2.303x/TVL})) \times 100 \quad \text{..... (11)}$$

$$\textbf{Protection Efficiency (PE, \%)} = (1-(e^{-0.693x/HVL})) \times 100 \quad \text{..... (12)}$$

$$\textbf{Protection Efficiency (PE, \%)} = (1-(e^{-x/MEP})) \times 100 \ldots\ldots\ldots (13)$$

To estimate the accuracy of PE% calculation by equation 10 compared to equation (11, 12, or 13), Percentage of Difference (Δ%, 14) was applied at 15 MeV (Table 11). All calculated Δ% values from equation 14 were less than 1% which reflects a high degree of agreement between all PE% calculations. These differences may be related to the approximation of (ln 10= 2.302585093 ≈ 2.303 or ln 2=0.6931471806 ≈ 0.693) (Table 11, equations (10-13)).

$$\Delta\% = (PE\%_{(equation10)} - PE\%_{(equation\ 11,\ 12,\ or\ 13)})/PE\%_{(equation\ 10)}) \times 100 \ldots\ldots\ldots (14)$$

Table (11): Percentage of Difference (Δ%) calculated from LAC and compared to TVL, HVL, or MEP data (NGCal model) at 15 MeV, x= 0.1 cm.

ID	PE% (10)	TVL. cm	PE% (11)	HVL, cm	PE% (12)	MEP, cm	PE% (13)	Δ%		
								TVL	HVL	MEP
S1	**2.3519**	**9.683**	2.3503	**2.915**	2.3493	**4.205**	2.3501	0.0666	0.1096	0.0779
S2	1.7151	**13.272**	1.7203	**3.995**	1.7197	**5.764**	1.7199	-0.3011	-0.2688	-0.2824
S3	2.7514	**8.259**	2.7500	**2.486**	2.7491	**3.587**	2.7493	0.0526	0.0830	0.0748
S4	2.6541	**8.562**	2.6539	**2.578**	2.6523	**3.719**	2.6531	0.0061	0.0670	0.0390
S5	2.4495	**9.29**	2.4485	**2.797**	2.4472	**4.035**	2.4479	0.0394	0.0934	0.0671
S6	2.586	**8.799**	2.5834	**2.649**	2.5822	**3.821**	2.5832	0.1010	0.1485	0.1096

4. Conclusions

In this study, different nickel alloys varied in their chemical formulas, mole fractions (%) of each element, density, and Mean Atomic Number ($\bar{Z}$), alongside other chemical-physical properties were tested as a shielding material by theoretical prediction study depending on NGCal and Phy-X attenuation factors against Neutron, Gamma radiation, and X-rays exposure. Linear Attenuation Coefficient (LAC), Mass Attenuation Coefficient (MAC), Half and Tenth Value Layer (HVL and TVL), and Mean Free Path (MFP) beside protection efficiency (%) of each nickel alloy were calculated. This study target choosing best shielding material among (Ni_3Al, NiAl, $Ni_{90}Cr_{10}$, $Ni_{80}Cr_{20}$, $Ni_{35}Cr_{20}Fe_{45}$, and $Ni_{60}Cr_{16}Fe_{34}$) and their basic elements to protect workers that deal with Neutron, Gamma radiation, and X-rays particularly in the research, medical, industrial, and petroleum sectors especially at high exposure energies. Here, protection efficiency; depends on LAC; exhibits numerical data that has high similarity and compatibility with PE% depending on TVL, HVL, or MEP. Both mathematical models indicated that Chromel ($Ni_{90}Cr_{10}$) as the highest density and high Nickel mole fraction was superior shielding that exhibited the highest protection efficiency against all tested rays and particles. In comparison with their basic elements and Lead, Nickel then Chromel were best shielding against thermal and fast neutrons while Pb > Ni > Chromel was the best shielding sequence against incident photons.

Conflict of Interest: The authors declare that there are no conflicts of interest associated with this research project. We have no financial or personal relationships that could potentially bias our work or influence the interpretation of the results.

References

[1] B. Aygün, "Neutron and gamma radiation shielding Ni based new type super alloys development and production by Monte Carlo Simulation technique", *Radiation Physics and Chemistry*, vol. 188, Article number 109630, 2021.

[2] B. Kanagaraj, N. Anand, A. Andrushia, and M. Naser, "Recent developments of radiation shielding concrete in nuclear and radioactive waste storage facilities – A state of the art review", *Construction and Building Materials*, vol. 404, Article number 133260, 2023.

[3] N. Tsoulfanidis and S. Landsberger, "Measurement and Detection of Radiation", CRC Press, USA, 2021.

[4] B. Aygün, " High alloyed new stainless steel shielding material for gamma and fast neutron radiation", *Nuclear Engineering and Technology*, vol. 52, no. 3, pp. 647-653, 2020.
[5] C. More, Z. Alsayed, M. Badawi, A. Thabet, and P. Pawar, " Polymeric composite materials for radiation shielding: a review", *Environmental Chemistry Letters*, vol. 19, pp. 2057–2090, 2021.
[6] C. Okafor, U. Okonkwo, and I. Okokpujie, "Trends in reinforced composite design for ionizing radiation shielding applications: a review", *Journal of Materials Science*, vol. 5, pp.11631–11655, 2021.
[7] D. Shi, Y. Xia, J. Wang, F. Chen, X. Ma, Y. Zhao, M. Liu, and K. Yu, "Recycling E-waste CRT glass in sustainable geopolymer concrete for radiation shielding applications", *Journal of Environmental Chemical Engineering*, vol. 12, Article number 114693, 2024.
[8] E. Kavaz, N. Ekinci, H. Tekin, M. Sayyed, B Aygün, and U. Perişanoğlu, " Estimation of gamma radiation shielding qualification of newly developed glasses by using WinXCOM and MCNPX code", *Progress in Nuclear Energy*, vol. 115, pp. 12-20, 2019.
[9] F. Akman, M. Kaçal, N. Almousa, M. Sayyed, and H. Polat, "Gamma-ray attenuation parameters for polymer composites reinforced with $BaTiO_3$ and $CaWO_4$ compounds", *Progress in Nuclear Energy*, vol. 121, Article number 103257, 2020.
[10] H. Bichsel and H. Schindler, "The interaction of radiation with matter. In *Particle Physics Reference Library Detectors for Particles and Radiation*", Vol. 2, Editors: C. Fabjan and H. Schopper, Springer, 2020.
[11] IARC Working Group on the Evaluation of Carcinogenic Risks to Humans. Ionizing Radiation, Part 1: X- and Gamma (γ)-Radiation, and Neutrons. Lyon (FR): International Agency for Research on Cancer; (IARC Monographs on the Evaluation of Carcinogenic Risks to Humans, No. 75.), 2000.
[12] K. Filak-Mędoń, K. Fornalski, M. Bonczyk, A. Jakubowska, K. Kempny, K. Woloszczuk, K. Filipczak, K. Żerańska, and M. Zdrojek, "Graphene-based nanocomposites as gamma- and X-ray radiation shield", *Scientific Reports*, vol. 14, Article number 18998, 2024.
[13] M. Akbar, B. Armynah, and D. Tahir, "Comprehensive compilation and analysis of wood composite materials for X-ray, Gamma-ray, and neutron radiation shielding applications: A review, " *Industrial Crops and Products*, Vol. 222, Article number 119440, 2024.
[14] N. AbuAlRoos, N. Amin, and R. Zainon, "Conventional and new lead-free radiation shielding materials for radiation protection in nuclear medicine: A review", *Radiation Physics and Chemistry*, vol. 15, Article number 108439, 2019.
[15] J. Wang, H. Zhou, Y. Gao, Y. Xie, J. Zhang, Y. Hu, D. Wang, Z. You, S. Wang, H. Li, G. Liu, and A. Mi, "The Characterization of Silicone-Tungsten-Based Composites as Flexible Gamma-Ray Shields." *Materials (Basel, Switzerland)*, vol. 14, no. 20, pp. 5970, 2021.
[16] N. AbuAlRoos, M. Azman, N. Amin, and R. Zainon, "Tungsten-based material as promising new lead-free gamma radiation shielding material in nuclear medicine", *Physica Medica*, vol. 78, pp. 48-57, 2020.
[17] Y. Wu, Y. Cao, Y. Wu, and D. Li, ‘'Mechanical Properties and Gamma-Ray Shielding Performance of 3D-Printed Poly-Ether-Ether-Ketone / Tungsten Composites", *Materials (Basel, Switzerland)*, vol. 13, no. 20, pp. 4475, 2020.
[18] S. Barbhuiya, B. Das, P Norman, and T. Qureshi, "A comprehensive review of radiation shielding concrete: Properties, design, evaluation, and applications", *Structural Concrete*, vol. 2024, pp. 1–47, 2024.
[19] T. Korkut, A. Karabulut, G. Budak, B. Aygün, O. Gencel, and A. Hançerlioğulları, "Investigation of neutron shielding properties depending on number of boron atoms for colemanite, ulexite and tincal ores by experiments and FLUKA Monte Carlo simulations ", *Applied Radiation and Isotopes*, vol. 70, pp. 341-345, 2012.
[20] V. Singh, N. Badiger, N. Chanthima, and J. Kaewkhao, "Evaluation of gamma-ray exposure buildup factors and neutron shielding for bismuth boro silicate glasses", *Radiation Physic and Chemistry*, vol. 98, pp. 14-21, 2014.
[21] V. Zali, O. Jahanbakhsh, and I. Ahadzadeh, "Preparation and evaluation of gamma shielding properties of silicon-based composites doped with WO_3 micro- and nanoparticles", *Radiation Physics and Chemistry*, vol. 197, Article number 110150, 2022.
[22] A. Acevedo-Del-Castillo, E. Águila-Toledo, S. Maldonado-Magnere, and H. Aguilar-Bolanos, ‘'A Brief Review on the High-Energy Electromagnetic Radiation-Shielding Materials Based on Polymer Nanocomposites", *International Journal of Molecular Sciences*, vol. 22, no. 16, pp. 9079, 2021

[23] B. Subedi, J. Paudel, and T. Lamichhane, "Gamma-ray, fast neutron and ion shielding characteristics of low-density and high-entropy Mg-Al-Ti-V-Cr-Fe-Zr-Nb alloy systems using Phy-X/PSD and SRIM programs", *Heliyon*, vol. 9, no. 7, Article number: e17725, 2023.

[24] C. Kursun, M. Gao, S. Guclu, Y. Gaylan, K. Parrey, and A. Yalcin, "Measurement on the neutron and gamma radiation shielding performance of boron-doped titanium alloy $Ti_{50}Cu_{30}Zr_{15}B_5$ via arc melting technique'', Heliyon, vol. 9, no. 11, Article number: e21696, 2023.

[25] I. Nabil, M. El-Samrah, A. Omar, A. Tawfic, and A. El Sayed, ''Experimental, analytical, and simulation studies of modified concrete mix for radiation shielding in a mixed radiation field", *Scientific Reports*, vol. 13, no. 1, pp. 17637, 2023.

[26] G. Lakshminarayan, Y. Elmahroug, A. Kumar, H. Tekin, N. Rekik, M. Dong, D. Lee, J. Yoon, and T. Park, "Detailed Inspection of γ-ray, Fast and Thermal Neutrons Shielding Competence of Calcium Oxide or Strontium Oxide Comprising Bismuth Borate Glasses", *Materials* (Basel, Switzerland), vol. 14, no. 9, pp. 2265, 2021.

[27] H. Tekin, S. Issa, G. Kilic, H. Zakaly, M. Abuzaid, N. Tarhan, K. Alshammari, H. Sidek, K. Matori, and M. Zaid, "In-Silico Monte Carlo Simulation Trials for Investigation of V_2O_5Reinforcement Effect on Ternary Zinc Borate Glasses: Nuclear Radiation Shielding Dynamics. *Materials (Basel, Switzerland)*, vol. 14, no. 5, pp. 1158. 2021.

[28] H. Gökçe, O. Güngör, and H. Yılmaz an online software to simulate the shielding properties of materials for neutrons and photons: NGCal", *Radiation Physics and Chemistry*, vol. 185, Article number 109519, 2021.

[29] E. Şakar, Ö. Özpolat, B. Alım, M.I. Sayyed, and M. Kurudirek, "Phy-X / PSD: Development of a user-friendly online software for calculation of parameters relevant to radiation shielding and dosimetry", *Radiation Physics and Chemistry* vol. 166, Article number 108496, 2020.

[30] Y. Wu, C. Li, Y. Li, J. Wu, X. Xia, and Y. Li, "Effects of heat treatment on the microstructure and mechanical properties of Ni_3Al-based superalloys: A review", *International Journal of Minerals, Metallurgy and Materials*, vol. **28**, pp. 553–566, 2021.

[31] M. Khomutov, P. Potapkin, V. Cheverikin, P. Petrovskiy, A. Travyanov, I. Logachev, A. Sova, and I. Smurov, "Effect of hot isostatic pressing on structure and properties of intermetallic NiAl–Cr–Mo alloy produced by selective laser melting", *Intermetallics*, vol. 120, Article number 106776, 2020.

[32] S. Vinayak, H. Vyas, and V. Vankar, "Microstructure and electrical characteristics of Ni–Cr thin films", *Thin Solid Films*, vol. 515, pp. 7109 -7116, 2007.

[33] T. Hüp, C. Cagran, E. Kaschnitz, and G. Pottlacher, " Thermophysical properties of $Ni_{80}Cr_{20}$", *Thermochimica Acta*, vol. 494, pp. 40 – 44, 2009.

[34] S. Agostinelli, J. Allison, K. Amako, J. Apostolakis, H. Araujo, P. Arce, M. Asai, D. Axen, S. Banerjee, G. Barrand, F. Behner, L. Bellagamba, J. Boudreau, L. Broglia, A. Brunengo, H. Burkhardt, S. Chauvie, J. Chu, R. Chytracek, G. Cooperman'', Geant4—a simulation toolkit", *Nuclear Instruments and Methods in Physics Research Section A: Accelerator, Spectrometers, Detectors and Associated Equipment*, vol. 506, no. 1, pp.250-303, 2003.

[35] K. Mann and S Mann, " Py-MLBUF: Development of an online-platform for gamma-ray shielding calculations and investigations", *Annals of Nuclear Energy*, vol. 15o, Article number 107845, 2021.

[36] F. Hila, A. Asuncion-Astronomo, C. Dingle, J. Jecong, A. Javier-Hila, M. Gili, C. Balderas, G. Lopez, N. Guillermo, and A. Amorsolo Jr., " EpiXS: A Windows-based program for photon attenuation, dosimetry and shielding based on EPICS2017 (ENDF/B-VIII) and EPDL97 (ENDF/B-VI.8)", *Radiation Physics and Chemistry*, vol. 182, Article number 109331, 2021.

[37] N. Salman and K. Hammud, "Phy-X/PSD and NGCAL Models of Several Metal Sulphides: Theoretical Prediction of Gamma Shielding Efficiency", *Iraqi Journal of Industrial Research, vol. 11, no.* 3, pp. 94–118, 2024.

[38] J. Zaidan", Natural Occurring Radioactive Materials (NORM) in the oil and gas industry", *Journal of Petroleum Researches and Studies*, vol. 1, no. 1, pp. 3-18, 2010.

[39] J. Popic, L. Urso, and B. Michalik, "Assessing the exposure situations with naturally occurring radioactive materials across European countries by means of the e-NORM survey", *Science of the Total Environment*, vol. 905, Article Number 167065, 2023.

[40] Xiong, Deming, and C. Wang. "Risk assessment of human exposure to heavy metals, polycyclic aromatic hydrocarbons, and radionuclides in oil-based drilling cutting residues used for roadbed materials in Chongqing, China." *Environmental Science and Pollution Research*, vol. 28, pp. 48171-48183, 2021.

[41] A. Al-Rubaye, D. Jasim, H. Al-Robai, H. Al-khafaj, H. Ameen, and A. Al-Turaihi, "Risks of Naturally Occurring Radioactive Material Exposure on the Environment in Oil and Gas Field", *IOP Conference Series: Earth and Environmental Science*, vol. 1371, Article number 022022, 2024.

[42] T. Elmahroug, and C. Souga", Investigation on radiation shielding parameters of cerrobend alloys", *Nuclear Engineering and Technology*, vol. 49, no. 8, pp. 1758 -1771, 2017.